[논 문] 한국재료학회지
Kor. J. Mater. Res.
Vol. 24, No. 1 (2014)
http://dx.doi.org/10.3740/MRSK.2014.24.1.6

Sonocatalytic Degradation of Rhodamine B in the Presence of TiO_2 Nanoparticles by Loading WO_3

Ze-Da Meng[1,2], Sourav Sarkar[2], Lei Zhu[2], Kefayat Ullah[2], Shu Ye[2] and Won-Chun Oh[2†]

[1]Jiangsu Key Laboratory of Environmental Functional Materials, College of Chemistry and Bioengineering, Suzhou University of Science and Technology, Suzhou 215009, China
[2]Department of Advanced Materials Science & Engineering, Hanseo University, Seosan-si, Chungnam-do 356-706, Korea

(Received September 12, 2013 : Received in revised form November 19, 2013 : Accepted November 27, 2013)

Abstract In the present work, WO_3 and WO_3-TiO_2 were prepared by the chemical deposition method. Structural variations, surface state and elemental compositions were investigated for preparation of WO_3-TiO_2 sonocatalyst. X-ray diffraction (XRD), scanning electron microscopy (SEM), energy dispersive X-ray (EDX) and transmission electron microscopy (TEM) were employed for characterization of these new photocatalysts. A rhodamine B (Rh.B) solution under ultrasonic irradiation was used to determine the catalytic activity. Excellent catalytic degradation of an Rh.B solution was observed using the WO_3-TiO_2 composites under ultrasonic irradiation. Sonocatalytic degradation is a novel technology of treating wastewater. During the ultrasonic treatment of aqueous solutions sonoluminescence, cavitaties and "hot spot" occurred, leading to the dissociation of water molecules. In case of a WO_3 coupled system, a semiconductor coupled with two components has a beneficial role in improving charge separation and enhancing TiO_2 response to ultrasonic radiations. In case of the addition of WO_3 as new matter, the excited electrons from the WO_3 particles are quickly transferred to TiO_2 particle, as the conduction band of WO_3 is 0.74 eV which is −0.5 eV more than that of TiO_2. This transfer of charge should enhance the oxidation of the adsorbed organic substrate. The result shows that the photocatalytic performance of TiO_2 nanoparticles was improved by loading WO_3.

Key words WO_3, ultrasonic, TEM, sonocatalyst, UV-Vis.

1. Introduction

The textile industry sector wastewaters contain excess dyes that cannot be (fully) removed via conventional biological treatment and the discharge of the resulted waters may cause long-term environmental problems.[1)] Photocatalysis represents a viable option for complete degrading the dye molecules to products that do not represent environmental threats, as reported by many papers.[2,3)]

Titanium dioxide is an intensively studied photocatalyst but it can only benefit of the UV region of the spectrum for wastewater treatment. This limits its efficiency due to the relative small percentage of UV light in the solar radiation received at the ground level (about 7…10 %) and rises the cost of the wastewater treatment process.[4)] Various solutions were developed to solve this problem, including doping and the development of TiO_2-based tandem systems. Recent studies show that coupling TiO_2 and WO_3, new types of nano-composite tandem materials are obtained with good catalytic activity.[5)]

The past few years have seen a dramatic rise in the applications of high-intensity, or power, ultrasound in chemistry, with a range of synthetic procedures and process methods having found to benefit from sonication. Sonocatalytic degradation is a novel technology of treating wastewater.[6)] During the ultrasonic treatment of aqueous solutions sonoluminescence, cavitational and "hot spot" were happened, leading to the dissociation of water molecules. The hydroxyl (OH) radicals were firmed during the ultrasonic treatment which has high oxidative activity can degradation the toxic dyes and industrial dyestuffs. One of the applications of ultrasound is for the polymer degradation.[7)] The technique of ultrasound, on the other hand, has received much attention as an advanced oxidation

†Corresponding author
E-Mail : wc_oh@hanseo.ac.kr (W.-C. Oh, Hanseo Univ.)

process for treating contaminants in water. When using ultrasound some complicate reactions can be performed with inexpensive equipment and often in fewer steps than with the conventional methods.[8)]

In this paper, we reported attempted to improve the photocatalytic performance of TiO_2 nanoparticles by loading WO_3. Structural variations, surface state and elemental compositions were investigated for preparation of WO_3-TiO_2 sonocatalyst. X-ray diffraction (XRD), scanning electron microscopy (SEM), energy dispersive X-ray (EDX) and transmission electron microscopy (TEM) were employed for characterization of these new photocatalysts. The sonocatalytic efficiencies of these composites were evaluated by the ultrasonic degradation of rhodamine B (RhB, $C_{28}H_{31}ClN_2O_3$) solutions.

2. Experimental

2.1 Materials

Benzene (99.5 %) and ethyl alcohol were purchased as reagent-grade from Duksan Pure Chemical Co. (Ansan-si, Gyeonggi-do, South Korea) and Daejung Chemical Co. (Gwangju-si, Gyeonggi-do, South Korea) and were used as received. Titanium-(IV) *n*-butoxide (TNB, $C_{16}H_{36}O_4Ti$) as the titanium source for the preparation of the WO_3-fullerene/TiO_2 composites was purchased as reagent-grade from Acros Organics (Morris Plains, NJ, USA). The ammonium metatungstate hydrate ($H_{26}N_6O_{40}W_{12}{\cdot}xH_2O$) purchased from Sigma-Aldrich^{TM} Chemie GmbH (Steinheim, Germany) was used asa raw material to generate WO_3 at high temperatures. Rhodamine B (RhB, $C_{28}H_{31}ClN_2O_3$, 99.9 %, Duksan Pure Chemical Co., Ltd) was of analytical grade.

2.2 Preparation of WO_3

For WO_3 coating, 3.8×10^{-5} mol $H_{26}N_6O_{40}W_{12}{\cdot}xH_2O$ was added to 50 ml of distilled water (shown in Table 1). The resulting mixture was heated under reflux in air and stirred at 343 K for 6h using a magnetic stirrer in a vial. After heat treatment at 773 K for 1h, the WO_3 compounds were formed.

2.3 Preparation of WO_3-TiO_2 composites

WO_3 was prepared using pristine concentrations of TNB for the preparation of WO_3-TiO_2 composites. WO_3 powder was mixed with 3 ml TNB. The solutions were homogenized under reflux at 343 K for 5 h, while being stirred in a vial. After stirring, the solution transformed to WO_3-TiO_2 gels and heat treated at 873 K to produce the WO_3-TiO_2 composites.

2.4 Characterization of photocatalysts compounds

To measure thestructural variations, XRD patterns were obtained using an X-ray generator (Shimadzu XD-D1, Shimadzu Corporation, Kyoto, Japan) with Cu Kα radiation. Scanning electron microscopy (SEM, JSM-5200, JEOL, Tokyo, Japan) was used to observe the surface state and structure of the photocatalyst composites. Energy dispersive X-ray spectroscopy (EDX) was also used for elemental analysis of the samples. Transmission electron microscopy (TEM, JEM-2010, JEOL) was used to observe the surface state and structure of the photocatalyst composites atan acceleration voltage of 200 kV. TEM was also used to examine the size and distribution of the titanium and iron particles deposited on the fullerene surface of various samples. The TEM specimens were prepared by placing a few drops of the sample solution on a carbon grid. UV-vis diffused reflectance spectra were obtained using a UV-vis spectrophotometer (Neosys-2000, Scinco, Seoul, South Korea) by using $BaSO_4$ as a reference and were converted from reflection to absorbance by the Kubelka-Munk method.

2.5 Ultrasonic degradation of dye solutions

Controllable Serial-Ultrasonic apparatus (Ultrasonic Processor, VCX 750, Korea) was adopted to irradiate the rhodamine B solution, operation at ultrasonic frequency of 20 kHz and output power of 750 W through manual adjusting. A specified quantity of photocatalysts composites were added to 90 ml pure water. To disperse the particles, the ultrasound was irradiated for 30min, after ultrasound treated, the reactor were become particle suspension. Then, the ultrasonic irradiation was once stopped and 10 ml rhodamine B solution (1.00×10^{-4} mol/L) was added to the particle suspension. The reactor was placedwas placed on the magnetic churn dasher, stirring for 120 minutes in the darkness box to establish an adsorption-desorption equilibrium. After the adsorption state, the ultrasonic irradiation was restarted to make the degradation reaction proceed. The initial concentration of the RhB was set at 1×10^{-5} mol/L in all experiments. The amount of the photocatalysts composite was 0.02 g/(100 ml solution). Controlling the temperature around room temperature (20.0 °C), the reactor was treated by water bath. In the process of degradation of Rhodamine B, a glass reactor (diameter = 5 cm, height = 7 cm) was used and the reactor was placed on the magnetic churn dasher. The diameter of ultrasonic tip is 1.90 cm, and the ultrasonic irradiation surface area is 26.86 cm^2. Ultrasonic irradiation of the reactor was done for 10 min, 30 min, 60 min, 90 min and 120 min, respectively. Samples (3 ml) were then withdrawn regularly from the reactor and removal of dispersed powders through a centrifuge. After treatment of centrifuge the centrifugalizations were analyzed by using a UV-vis spectrophotometer. As the catalytic properties of photocatalysts composition absorption and

degradation the blue color of the solution faded gradually with time.

3. Results and Discussion

3.1 Elemental analysis of the preparation

Fig. 1 shows the EDX investigations for the WO_3-TiO_2 compounds. The elemental composition of these samples has been analyzed and the characteristic elements were identified using an EDX detection spectrometer. Fig. 1 shows that strong Kα and Kβ peaks from Ti element appear at 4.51 and 4.92 keV, while a moderate Kα peak of the element O appears at 0.52 keV.[9] EDX indicated O, Ti, and W as the major elements in the composites. Fig. 1 shows the presence of O, and Ti, as major elements with strong W peaks. Fig. 1(b) is the element weight percentage of WO_3-TiO_2 compounds.

3.2 Surface characteristics of the samples

The micro-surface structures and morphologies of the composites were characterized by SEM (Fig. 2). The SEM technique is used for inspecting topographies of specimens at very high magnifications using a piece of equipment called the scanning electron microscope. Fig.

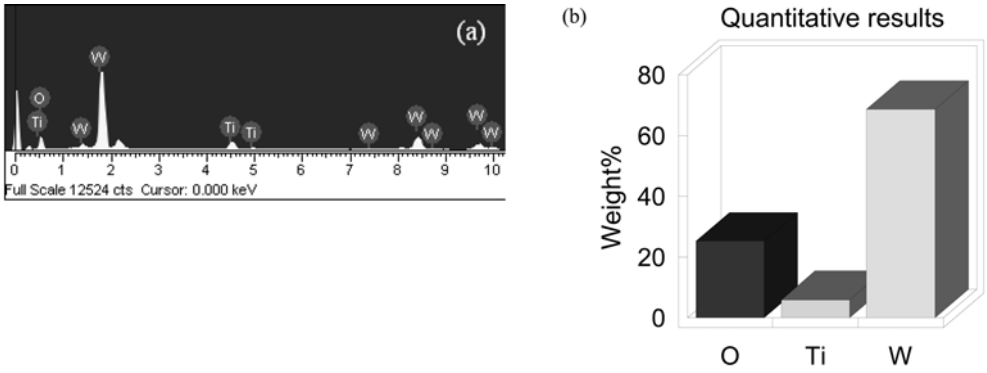

Fig. 1. EDX microanalysis and element weight percentage of WO_3-TiO_2.

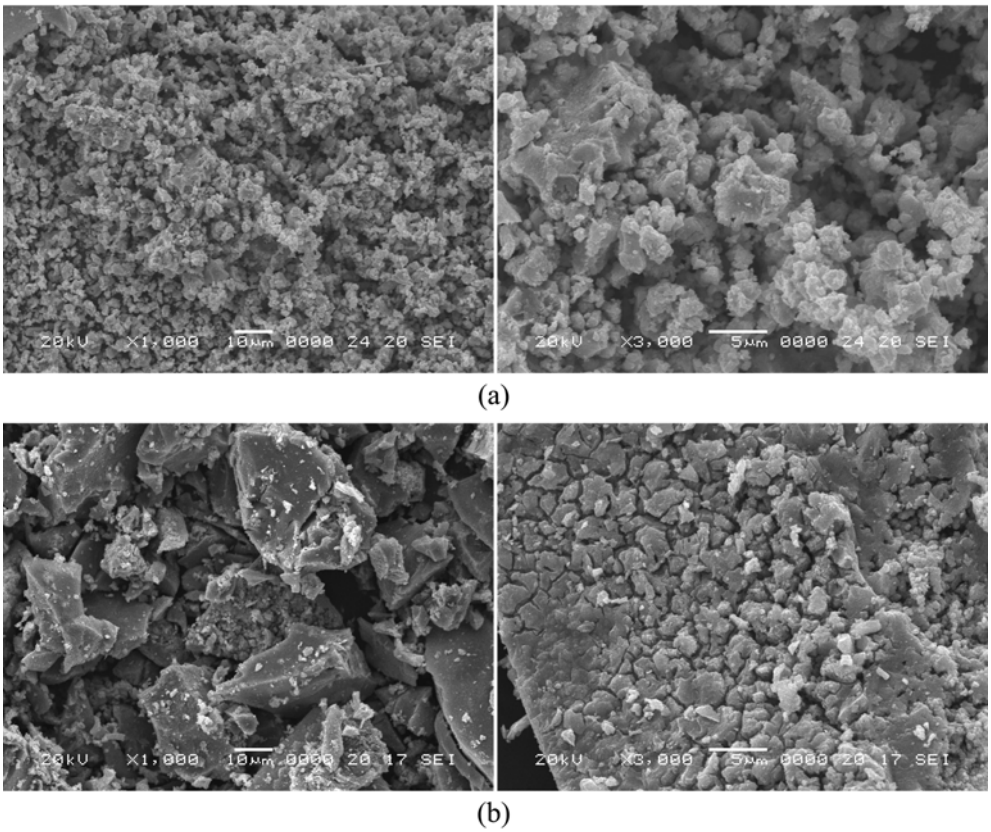

Fig. 2. SEM microanalysis of WO_3 (a) and WO_3-TiO_2 (b).

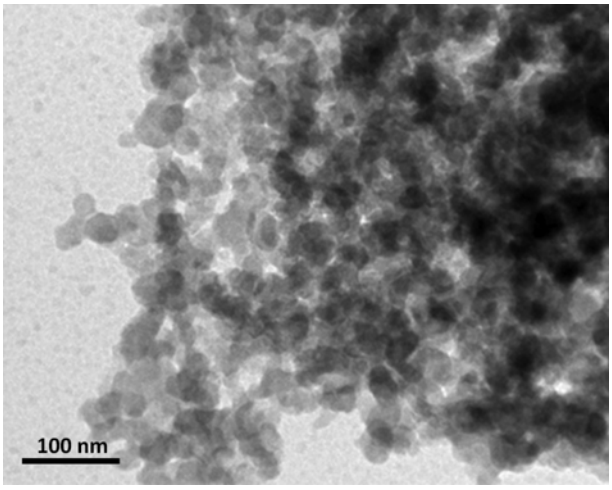

Fig. 3. TEM image obtained from WO_3-TiO_2 composites.

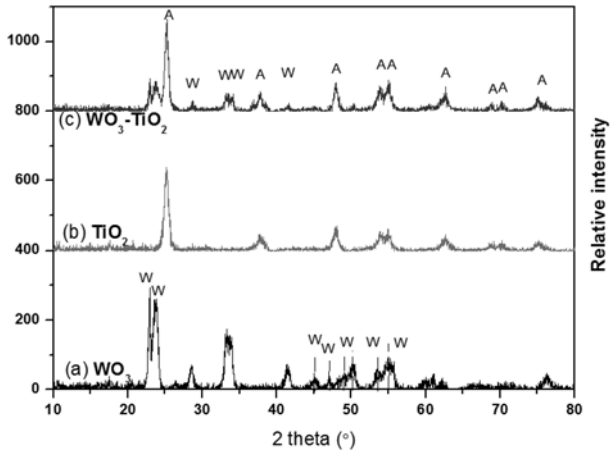

Fig. 4. XRD patterns from samples.

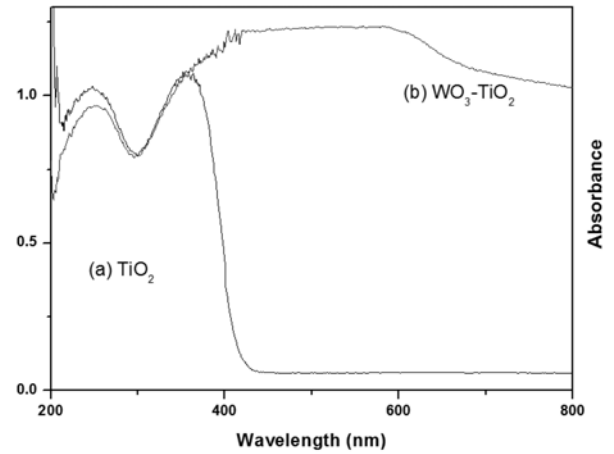

Fig. 5. UV-vis absorption spectra of photocatalysts.

2 shows the macroscopic changes in the morphology of the composites. In Fig. 2 WO_3 have a small particle size and a good dispersion. Zhang et al. reported that a good dispersion of small particles could provide more reactive sites for the reactants than aggregated particles.[10] Comparing WO_3 and WO_3-TiO_2 samples (Fig. 2(a, and b)), tungsten oxide particles were fixed to the TiO_2 surface and the distribution was uniform, but the particles were more numerous and larger than those of pure WO_3. The particle size of WO_3 becomes larger after loading TiO_2. By comparing Fig. 2(a) and (b), after added TiO_2, the dispersion of WO_3 has a little deteriorated.

Fig. 3 shows TEM images of the WO_3-TiO_2 composites. TEM is a technique used for analyzing the morphology, crystallographic structure, and even the composition of a specimen. Fig. 3 gives direct evidence that the WO_3 are well contact with TiO_2. As shown in Fig. 3, particles were observed upon enlargement of the images. This indicates that the surfaces of the WO_3 particles are cleaned under exposure to the reaction conditions. WO_3 particles were uniform distributed on the surface of TiO_2. The size of WO_3 and TiO_2 were approximately 35 nm.

3.3 Structural analysis

XRD was used to determine the crystallographic structure of the inorganic component of the composite. Fig. 4 shows the XRD patterns of the WO_3, TiO_2, and WO_3-TiO_2. In Fig. 4, A is anatase and W is the monoclinic phase of tungsten oxide. The peaks at 23.15°, 23.61°, 24.37°, 26.61°, 33.33°, 33.65°, 34.01°, 41.51°, 44.88°, 47.22°, 49.32°, 50.48°, 53.46°, and 55.11°, 2θ were assigned to diffraction planes of (001), (020), (200), (120), (111), (021), (201), (220), (221), (131), (002), (400), (112), (022) and (401) of monoclinic WO_3 phase.[11,12] The crystal structure of TiO_2 is determined mainly by the heat treated temperature. The peaks at 25.3°, 37.5°, 48.0°, 53.8°, 54.9°, and 62.5° 2θ were assigned to the (101), (004), (200), (105), (211), and (204) planes of anatase.[13,14] From the XRD patterns (Fig. 4), it is also possible to compute the % crystallinity and crystallite size. The amorphous phase fraction of the sample may be determined by taking the ratio of the amorphous area (area not under the peaks) of the X-ray diffractogram to the total area. Also the peaks at different crystal planes of WO_3-TiO_2 nanocomposite matches exactly with that of WO_3 indicating essentially no difference with respect to the type of crystalline phase in the two products. It is found that WO_3 shows more crystallinity than prepared WO_3-TiO_2. nanocomposite. This is attributed to the adverse environments created when added TiO_2, not allowing the nucleation and crystal growth to occur fully.[15]

The optical property of the as-prepared samples was studied by measuring their UV-vis absorption. Fig. 5 shows the UV-vis absorption spectra of TiO_2 and WO_3-TiO_2 samples. The spectral lines of two samples exhibit only one characteristic absorption band, which is assigned to the intrinsic transition from the valence band to the

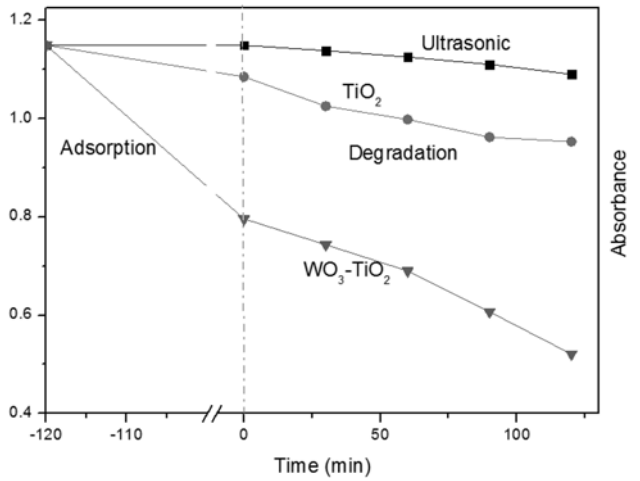

Fig. 6. Effect of the decolorization effect for Rh.B for sonocatalyst.

conduction band. As can be observed, the TiO_2 sample only shows light absorption in the UV region with its band gap transition at wavelength lower than ~400 nm. Unlike WO_3-TiO_2 composite exhibits a new and broad band gap with adsorption onset ~560 nm. The previous work demonstrated that this material is able to generate more than one electron-hole pair per high energy photon absorbed. Therefore, although the optical band gap is positioned at the near-infrared region, WO_3-TiO_2 composite can be still excited by the visible-light whose energy is higher than that of the optical band gap.[16] Because of the synergistic reaction of WO_3 and TiO_2, the adsorption effect of WO_3-TiO_2 is good in both the ultraviolet and visible regions.[17]

3.4 Degradation effects of the RhB

In Fig. 6, it is observed that the time series of RhB degradation using TiO_2, and WO_3-TiO_2 under ultrasonic irradiation. From these spectra for the RhB solution after ultrasonic irradiate, the relative yields of the degradation produce formed at different irradiation time conditions are shown for the products. Then the reduction of the dye concentration is continued with an oppositely gentle slope which is due to ultrasonic irradiation. The concentration of RhB is 1.0×10^{-5} mol/l, the absorbance for RhB decreases as the ultrasonic irradiation time increase. Moreover, the RhB solution increasingly loses its color, and its concentration continues to diminish. From Fig. 6, we compare the decontamination effect between ultrasonic, pure TiO_2, and WO_3-TiO_2. There are two steps during the decontamination process, one is adsorption, and another one is degradation.

When ultrasonic irradiate the solution, the waves through liquid medium in the generation of many cavities. This leads to develop high temperatures and high pressures within the cavities during their collapse. The consequences of these extreme conditions are the cleavage of dissolved oxygen molecules and water molecules into ·OH and ·Hradicals. The reactions of these entities with each other and with H_2O and O_2 yield the products of ·O and ·OH radical, so the organic compounds are decomposed and inorganic compounds are oxidized and reduced.[18] However, only ultrasonic irradiation to generate positive hole is limitedly.[19] The absorbance of RhB solution is decreased 5.13 % with only ultrasonic irradiate. When used the pure TiO_2, the adsorption effect and degradation effect is better, the absorbance of Rh. B solution is decreased 21.59 % after adsorption 120 minutes, and is decreased 23.75 % after ultrasonic irradiate 120 min.

In general, the occurrence of sonocatalytic degradation of organic pollutants in the presence of sonocatalyst isconsidered to be base upon the following three points of view, namely, sonoluminescence, “hot spot” and oxygen atom escape.

Sonoluminescence can occur when a sound wave have sufficiently intensity and induces a gaseous cavity within a liquid to collapse quickly. This cavity may take the form of a pre-existing bubble, or may be generated through a process known as cavitations. Sonoluminescence in the laboratory can be made to be stable, so that a single bubble will expand and collapse over and over again in a periodic fashion, emitting a burst of light each time it collapses. Because of sonoluminescence effect of ultrasonic irradiation, so in the ultrasonic irradiation process generated a lot of generated light. It has been well known that the ultrasonic irradiation can result in the formation of the light with a comparatively wide wavelength range because of acoustic cavitation. Those lights wavelengths are below 375 nm, beyond all doubt, can excite the TiO_2 particle acting as a photocatalyst and a great deal of ·OH radicals with high oxidation activity should form on the surface of the TiO_2 particles. In fact, that is the reaction mechanism of photocatalytic degradation. Be similar to the photocatalytic degradation, the sonocatalytic method also needs to restrain the recombination of electron-hole pair.

Usually, when sonochemical reaction pathways for the degradation of organic compounds by the sonolysis, at the first water as the solvent inside the collapsing cavitation bubbles under extremely high temperature and pressure (equation 1).[20] When added sonocatalytic, the ultrasonic dynamics system not only sonolysis of water but also coupled with induced by the catalyst to produce electron-hole pairs (equation 2). The electron-hole pairs can produce ·OH radical and superoxide anion $\cdot O_2$-, which can decompose the dyes to CO_2, H_2O and inorganic (equation 3, 4 and 5).[21]

$$H_2O + \text{Ultrasonic} \rightarrow \cdot OH + \cdot H \quad (1)$$

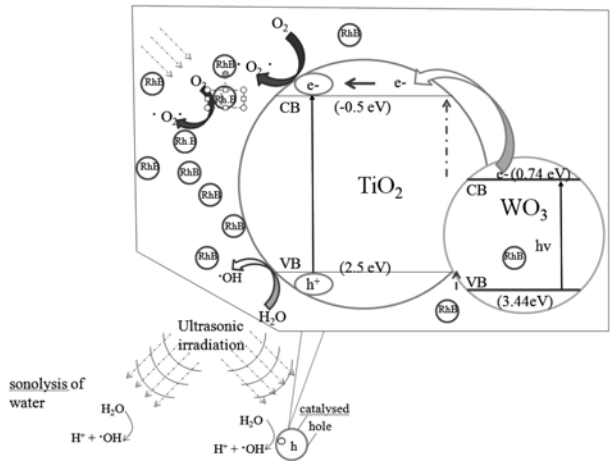

Fig. 7. Schematic drawing of separation of generated electrons and holes on the interface of CdS-C_{60}/TiO_2 compounds under ultrasonic irradiate.

$$\text{Sonocatalyst} + \text{Ultrasonic} \rightarrow e^- + h^+ \quad (2)$$

$$e^- + O_2 \rightarrow \cdot O_2\text{-} \quad (3)$$

$$h^+ + H_2O \rightarrow \cdot OH \quad (4)$$

$$\text{I-Rh. B} + \text{Sonocatalyst} + H_2O + O_2 + \text{Ultrasonic} \rightarrow CO_2 + H_2O + \text{inorganic} \quad (5)$$

We propose a mechanism for the degradation of pollutants on CdS-C_{60}/TiO_2 sonocatalyst under ultrasonic irradiation as shown in Fig. 7. The illustration is the mechanism for the degradation of pollutants on CdS-C_{60}/TiO_2 interface.

In case of WO_3 coupled system, semiconductor coupled with two components has a beneficial role in improving charge separation and enhance TiO_2 in response to ultrasonic. In case of addition of WO_3 as a new matter, the excited electron from the WO_3 particles are quickly transferred to TiO_2 particle due to the conduction band of WO_3 is 0.74 eV which is −0.5 eV more than that of TiO_2.[22-24] While the electrons formation excited from CdS are injected into the conduction band of TiO_2 and then scavenged by molecular oxygen O_2 toproduce the superoxide radical anion $\cdot O_2$-. This transfer of change should enhance the oxidation of the adsorbed organic substrate.

4. Conclusions

The nanoparticles of WO_3 and WO_3-TiO_2 composites were obtained by chemical deposition method. XRD result shows that titanium dioxide is in the form of anatase phase. Monoclinic phase of tungsten oxidecan find clearly, and introduce of TiO_2 prevent the growth of crystal. TEM image shows WO_3 and TiO_2 particles clearly. The high catalytic efficiency is attributed to the loading of WO_3 particles, which is helpful to effectively separate the generated carriers and to improve the surface properties of catalysts. Undoubtedly, the novel nanocomposites could provide an alternative pathway for the production of environmentally benign sonocatalysts exclusive for ultrasonic irradiate activation.

References

1. X. Chen and S.S. Mao, Chem. Rev., **107**(7), 2891 (2007).
2. C. Burda, Y. Lou, X. Chen, A. Samia and J. Stout, J. Gole, Nano Lett., **3**(8), 1049 (2003).
3. O. K. Dalrymple, E. Stefanakos, M. A. Trotz and D. Y. Goswami, Appl. Catal. B: Environ., **98**(1-2), 27 (2010).
4. K. K. Akurati, A. Vital, J. P. Dellemann, K. Mitchalow and T. Graule, Appl. Catal. B, **79**, 53 (2008).
5. S. Somasundaram, N. Tacconi, C. R. Chenthamarakshan and K. Rajeshwar, J. Electroanal. Chem., **57**(2), 167 (2005).
6. Z. D. Meng, L. Zhu, J. G. Choi, C. Y. Park and W. C. Oh, Nanoscale. Res. Let., **6**, 459 (2011).
7. J. Wang, W, Sun, Z. H. Zhang, Z. Q. Xing, R. Xu, R. H Li, Y. Li and X. D. Zhang, Ultrason. Sonochem., **15**(4), 301 (2008).
8. M. Kubo, K. Matsuoka, A. Takahashi, N. Shibasaki-Kitakawa and T. Yonemoto, Ultrason. Sonochem., **12**(4), 263 (2005).
9. D. Ke, H. Liu, T. Peng, X. Liu and K. Dai, Mater. Lett., **62**, 447 (2008).
10. X. W. Zhang, M. H. Zhou and L. C. Lei, Carbon, **43**(8), 1700 (2005).
11. S. F. Chen, L. Chen, S. Gao, and G. Y. Cao, Pow. Technol., **160**, 198 (2005).
12. L. M. Bertus, R. A. Carcel and A. Duta, Environ. Eng. Manage. J., **17**(10), 1021 (2011).
13. H. Liu, X. N. Dong, X. C. Wang, C. C. Sun, J. Q. Li and Z. F. Zhu, Chem. Eng. J., **230**(1-3), 279 (2013)
14. P. Xu, T. Xu, J. Lu, S. M. Gao, N. S. Hosmane, B. B. Huang, Y. Dai and Y. B. Wang, Energy Environ. Sci.. **3**(8), 1128 (2010).
15. S. Bagwasi, B. Z. Tian, J. L. Zhang, M. Nasir, Chem. Eng. J., **217**(5), 108 (2013).
16. P. Cheng, Z. Yang, H. Wang, W. Cheng, M. Chen, W. Shangguan, G. Ding, Inter.J. Hydr. Ener., **37**(3), 2224 (2012).
17. R. A. Carcel, L. Andronic, A. Duta, J. Nanosci. Nanotechnol., **11**(10), 9095 (2011).
18. Y. Segura, R. Molina, F. Martinez and J. A. Melero, Ultrason. Sonochem., **16**(3), 417 (2009).
19. M. H. Entezari and Z. Sharif Al-Hoseini, Ultrason. Sonochem., **14**(5), 599 (2007).
20. J. Saien, H. Delavari and A. R. Solymani, J. Hazar. Mate., **177**(1-3), 1031 (2010).

21. N. Wang, L. H. Zhu, M. Q. Wang, D. L. Wang and H. Q. Tang, Ultrason. Sonochem., **17**(1), 78 (2010).
22. J. Wang, Z. Jiang, L.Q. Zhang, P. L. Kang, Y. P. Xie, Y. H. Lv, R. Xu and X. D. Zhang, Ultrason. Sonochem., **16**(2), 225 (2009).
23. Tryba B, Piszcz M, Morawski AW. Int. J. Photoenergy., **01**, 15 (2009).
24. B. L. Abrams, J. P. Wilcoxon, Crit. Rev. Solid. State. Mater. Sci., **30**(3), 153 (2005).